Development 137, 2427-2437 (2010) doi:10.1242/dev.052605

Crooked, Coiled and Crimpled are three Ly6-like proteins required for proper localization of septate junction components

Anna Nilton[1,*], Kenzi Oshima[2,*], Fariba Zare[1,*], Sunitha Byri[1], Ulf Nannmark[1], Kevin G. Nyberg[2], Richard G. Fehon[2,†] and Anne E. Uv[1,†]

SUMMARY

Cellular junction formation is an elaborate process that is dependent on the regulated synthesis, assembly and membrane targeting of constituting components. Here, we report on three *Drosophila* Ly6-like proteins essential for septate junction (SJ) formation. SJs provide a paracellular diffusion barrier and appear molecularly and structurally similar to vertebrate paranodal septate junctions. We show that Crooked (Crok), a small GPI-anchored Ly6-like protein, is required for septa formation and barrier functions. In embryos that lack Crok, SJ components are produced but fail to accumulate at the plasma membrane. Crok is detected in intracellular puncta and acts tissue-autonomously, which suggests that it resides in intracellular vesicles to assist the cell surface localization of SJ components. In addition, we demonstrate that two related Ly6 proteins, Coiled (Cold) and Crimpled (Crim), are required for SJ formation and function in a tissue-autonomous manner, and that Cold also localizes to intracellular vesicles. Specifically, Crok and Cold are required for correct membrane trafficking of Neurexin IV, a central SJ component. The non-redundant requirement for Crok, Cold, Crim and Boudin (Bou; another Ly6 protein that was recently shown to be involved in SJ formation) suggests that members of this conserved family of proteins cooperate in the assembly of SJ components, possibly by promoting core SJ complex formation in intracellular compartments associated with membrane trafficking.

KEY WORDS: Trachea, Vesicles, Blood-brain barrier, GPI, *Drosophila*

INTRODUCTION

The multiprotein complexes of cellular junctions consist of membrane-spanning proteins, cytoplasmic scaffolding proteins and extracellular membrane-associated proteins that colocalize at specific sites along the lateral cell surface. Various mechanisms are presumably needed to ensure correct complex formation, including the attachment of cell adhesion molecules to cytoskeletal scaffolding proteins, membrane clustering of junction proteins by lateral interactions, and selective trafficking of vesicles to and from the site of junction assembly.

In *Drosophila*, the most prominent junctions are the pleated septate junctions (SJs). These are rows of protein assemblies found at the lateral cell surface (basal to the zonula adherens) of ectodermal-derived epithelia and between glial cells of the nervous system, and they appear as ladder-like intermembrane bands in electron micrographs (Stork et al., 2008; Tepass et al., 2001). An important function of SJs is to provide a barrier to paracellular diffusion. Epithelial SJ formation commences at mid-embryogenesis, after cell polarization and formation of the adherens junctions, and initially appears as single or small groups of septa. Additional septa are then added until the ladder-like bands cover one- to two-thirds of the lateral cell surface at stage 16 (Tepass and Hartenstein, 1994).

[1]Institute of Biomedicine, Göteborg University, Gothenburg, SE-40530, Sweden. [2]Department of Molecular Genetics and Cell Biology, University of Chicago, 920 East 58th Street, Chicago, IL 60637, USA.

*These authors contributed equally to this work
†Authors for correspondence (rfehon@uchicago.edu; anne.uv@medkem.gu.se)

Accepted 5 May 2010

Several proteins required for SJ formation have been identified, and these show a high degree of interdependence for their junctional localization. A core SJ complex consists of the three cell adhesion molecules Neurexin IV (Nrx-IV), Contactin (Cont) and Neuroglian (Nrg), and interacts via the Nrx-IV cytoplasmic tail with the cytoplasmic FERM domain protein Coracle (Cora) (Faivre-Sarrailh et al., 2004; Genova and Fehon, 2003; Tepass et al., 2001; Ward et al., 1998). An analogous protein complex, consisting of the cell adhesion molecules NCP1, NF-155, Contactin and the scaffolding protein 4.1B, is required for formation of the vertebrate paranodal septate junction, providing evidence for a molecular and functional conservation of these junctions (Banerjee et al., 2006; Girault and Peles, 2002; Tepass et al., 2001). *Drosophila* SJs also include two claudin-related tetraspan proteins, Sinuous (Sinu) and Megatrachea (Mega; Pickel – FlyBase) (Behr et al., 2003; Wu et al., 2004), the homophilic cell adhesion protein Lachesin (Llimargas et al., 2004), the Na,K-ATPase (Genova and Fehon, 2003; Paul et al., 2003) and a cytoplasmic MAGUK protein called Varicose (Vari) (Wu et al., 2007). However, the composition of the SJs is only partially defined, and how the components come together to form arrays of septa with paracellular fence function is not clear.

Many SJ components have been identified through studies of the developing embryonic trachea (respiratory organ), a network of epithelial tubes that spans the entire organism. In embryos with disrupted SJ components, the main tracheal tubes, the dorsal trunks, become excessively elongated (Wu and Beitel, 2004). The tube size defect could be ascribed to a need for SJs in the apical secretion of proteins that have functions in tube size regulation (Moussian et al., 2006; Wang et al., 2006).

In search of components required for SJ formation, we screened for new tracheal tube size genes and identified *crooked* (*crok*), a Ly6-like gene essential for SJ formation. A recent study has identified another member of the Ly6 gene family, *boudin* (*bou*), which is involved in SJ formation (Hijazi et al., 2009). Bou accumulates in the cytoplasm, but is also secreted and can support SJ assembly in a non-cell-autonomous manner (Hijazi et al., 2009). We show that Crok is needed for septa formation, the membrane accumulation of SJ components and paracellular barrier functions. Crok accumulates in cytoplasmic puncta that probably represent intracellular vesicles but, unlike Bou, Crok is required tissue-autonomously for SJ formation. The finding that two Ly6 proteins are required for SJ assembly, prompted us to survey additional Ly6 genes for a role in SJ formation. Functional analyses revealed two genes, *crimpled* (*crim*) and *coiled* (*cold*), that are expressed in the ectoderm and are required tissue-autonomously for SJ assembly, demonstrating that four Ly6-like proteins have selective and non-redundant functions in SJ assembly. A detailed analysis of Cold shows that this protein also accumulates in intracellular vesicles. Moreover, we find that Crok and Cold affect the intracellular trafficking of Nrx-IV, and propose that they have specific roles in the assembly or maintenance of the core Nrx-IV-containing SJ complex.

MATERIALS AND METHODS

Fly stocks and genetics

$crok^{KG06053}$ was obtained from Bloomington Drosophila Stock Center (BDSC, Indiana, USA) and is reported to carry two P-element insertions: *KG06053a* within *CG17218* (corresponding to C^{29} of Crok) and *KG06053b* within the *pipsqueak* (*psq*) gene. We could not detect *KG06053b* by PCR amplification of genomic DNA, and the tracheal phenotype and lethality was retained when $crok^{KG06053}$ was placed in trans to *Df(2L)esc-P3-0*, which uncovers *crok*, but not when it was placed in trans to *Df(2R)stan1*, which uncovers *psq*. Excision of *KG06053a* yielded five lethal *crok* mutant alleles and three lines in which lethality and tracheal phenotypes were rescued.

P{Mae-UAS.6.11}bou^{GG01077}, *l(1)air7*^{28}*/Dp(1;Y)ct*$^{+}$*y*$^{+}$*/FM7* (which uncovers *bou*), *PBac{WH1}CG2813*^{f05607} and *PBac{WH1}CG2813*^{f02238} (which are located in the first intron of *CG2813*), and the deficiency lines listed in Fig. 5 were obtained from BDSC. UAS-RNAi lines were obtained from the Vienna Drosophila RNAi Center (VDRC; Vienna, Austria): 44197 (*CG2813*), 44198 (*CG2813*), 44880 (*CG6583*), 11746 (*CG6583*), 30379 (*CG6038*) and 5443 (*CG14430*). Their expression was driven in tracheal cells from stage 11 using *btl-Gal4*.

The *UAS-crok* and *UAS-cold* constructs contain the *crok* (*CG17218*) or *cold* (*CG2813*) open reading frame from RE26906 or LD16147, respectively. In *UAS-crok-GFP*, the GFP coding sequence was inserted after position I^{24} in the Crok protein. The two *UAS-crok-FLAG* lines contain the epitope sequence DYKDDDDK after K^{25} (with the endogenous IK duplicated on either side) or after W^{27} (with the endogenous IKCW duplicated on either side), and the FLAG was flanked by single glycine residues. In the *UAS-cold-FLAG* construct, the DYKDDDDK sequence was inserted after position F^{121}. Germline transformations were carried out by BestGene or the Duke University Model Systems Genomics facility.

The GFP-tagged Nrx-IV line (Carnegie protein trap collection) contains a GFP-encoding exon inserted within an intron in the *Nrx-IV* locus (Buszczak et al., 2007). This insertion line is homozygous viable, suggesting that the tagged protein is fully functional.

Immunohistochemistry, dextran dye assays and TEM

Embryos were fixed with 4% formaldehyde for 20 minutes, except when using anti-Arm, anti-Baz and anti-Sinu, for which heat-methanol fixation was used. Primary antibodies used were: mouse monoclonal IgM 2A12 (1:10, Developmental Studies Hybridoma Bank, DSHB), rabbit anti-GFP (1:500; Molecular Probes), guinea pig anti-Cora (1:2000) (Fehon et al., 1994), mouse IgG anti-Atpα (1:10, DSHB), rabbit anti-Nrx-IV (1:500, from S. Baumgartner, Lund University, Sweden) mouse IgG1 monoclonal anti-Crb (1:10; DSHB), mouse monoclonal IgG2a anti-Fas3 (1:10; DSHB), rabbit anti-Sinu (1:500, from G. Beitel, Northwestern University, IL, USA), mouse anti-Arm (1:10, DSHB), rabbit anti-Baz (1:1000, from A. Wodarz, Georg-August-University, Germany) and rabbit anti-Knk (from B. Moussian, Tübingen University, Germany). Alexa-conjugated secondary antibodies (Molecular Probes or Jackson ImmunoResearch) were used at dilutions of 1:500 to 1:1000. Labelling with the Fluorescein-conjugated Chitin-binding Probe (1:500, New England Biolabs) was performed according to the manufacturer's recommendations.

UAS-cold-FLAG was transfected into S2 cells with dimethyldioctadecylammonium bromide (DDAB) (Han, 1996). Two days after transfection, cells were transferred onto Con-A-coated coverslips and cultured for 15 minutes. After adding a 10-kDa dextran conjugated with a tetramethylrhodamine dye (Molecular Probes) to the medium (final concentration 100 μg/ml), cells were incubated for 1.5 hours, fixed with 4% paraformaldehyde for 10 minutes and stained with mouse anti-FLAG (M2, 1:10,000, Sigma-Aldrich).

Crok antisera were generated by Inbio (Tallinn, Estonia) by co-injecting two peptides, CRKIRQKVHGEWRYFRS (amino acids 68-84) and CAYMGEPGIEGDERF (amino acids 85-99), into rabbits. The antisera were affinity-purified on columns covalently linked to either peptide, and were used at a dilution of 1:100.

The dextran dye permeability assay was performed as previously described (Lamb et al., 1998). Embryos were analyzed 20 minutes after injection. To label the endocytic and recycling vesicles, embryonic epidermis was observed one and half hours after injection of the fluorescent dextran dye. Confocal imaging was performed using either a Bio Rad Radiance 2000 system or a Zeiss LSM510 microscope. A Nikon eclipse E1000 microscope was used for obtaining wide-field fluorescence images. Early-stage 16 wild-type and *crok* mutant embryos were prepared for TEM as previously described (Tonning et al., 2005).

Western blot

Twenty stage 15 *crok/crok* or *crok/CyO* embryos were crushed in 20 μl sample buffer, the protein separated on a 15% SDS-PAGE gel and blotted onto a PVDF-membrane. The primary antisera, anti-Crok (1:1000), anti-Nrx-IV (1:5000), anti-ATPα (1:100) and anti-α-tubulin (Sigma, 1:10,000), were detected with HRP-conjugated secondary antibodies.

In situ hybridization

Whole-mount in situ hybridization was performed with digoxigenin-labelled RNA probes as previously described (Tonning et al., 2005). RNA probes were generated from genomic DNA templates amplified with primers containing T7 and T3 polymerase sequences (see Table S1 in the supplementary material), except for *crok,* when cDNA RE26906 was used as template for in vitro transcription. The *crok* probe was hydrolyzed to generate 0.5 kb fragments.

RESULTS

crooked is a new tracheal tube size gene

We searched for new tracheal tube size mutants by analysing available transposon-insertions in genes expressed in the embryonic trachea (according to the Berkeley Drosophila Genome Project, BDGP) (Tomancak et al., 2002). Using this strategy, we identified a mutant that we called *crooked* (*crok*), owing to its excessively long and convoluted tracheal dorsal trunks (Fig. 1A,B). *crok* mutants are reported to carry a P-element insertion allele, $CG17218^{KG06053}$, in the second protein-coding exon of *CG17218*, and by genomic sequencing we confirmed the position of the $CG17218^{KG06053}$ P-element insertion. The tracheal tube size defects and lethality are also detected in embryos transheterozygous for $CG17218^{KG06053}$ and *Df(2L)esc-P3-0*, which uncovers *CG17218* (Fig. 1C). Moreover, excision of the $CG17218^{KG06053}$ P-element yielded viable lines with normal trachea, indicating that the P-element insertion causes the tracheal phenotype and lethality of *crok* mutants. To confirm that

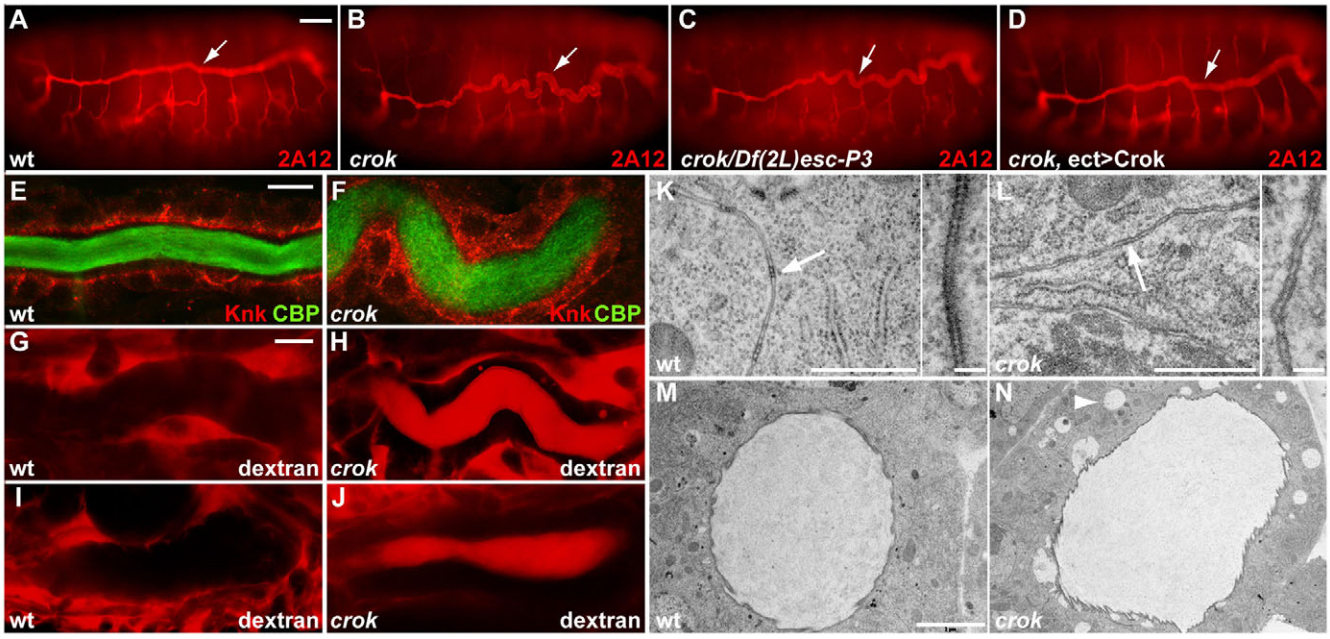

Fig. 1. Crooked is required for tracheal tube size regulation and SJ formation. (**A-D**) Stage 16 embryos labelled with the tracheal lumen-specific antibody 2A12. The dorsal trunk lumen (arrow) is elongated and convoluted in $crok^{KG06053}/crok^{KG06053}$ (B) and $crok^{KG06053}/Df(2L)esc\text{-}P3$ (C) embryos, compared with the wild type (A). The defect is rescued by expression of *UAS-crok* driven by *69B* Gal4 (ect>Crok, D). (**E**,**F**) The luminal chitin matrix, visualized by a chitin-binding protein (CBP, green), appears filamentous in the wild type (E), but wider and amorphous in $crok^{KG06053}$ mutants (F). Knk (red) is apical in the wild-type trachea (E), but mislocalized along the lateral and basal surfaces in *crok* mutants (F). (**G-J**) The 10-kDa Rhodamine-conjugated dextran injection into the body cavity is excluded from the tracheal (G) and salivary gland (I) lumens in wild type, but not in $crok^{KG06053}$ mutants (H,J). (**K-N**) Transmission electron microscopy (TEM) of tracheal cross-sections from wild-type stage 16 embryos reveals regularly spaced septa connecting the lateral membranes of adjacent cells (arrow and inset in K). The septa are sparser and less electron dense in *crok* mutants (arrow and inset in L). *crok* mutants also display irregular lumen diameter and large intracellular vesicles (arrowhead, N) that are not seen in the wild type (M). Scale bars: in A, 25 μm; in E, 5 μm; in G, 5 μm; in K,L, 0.5 μm; in insets in K,L, 0.1 μm; in M,N, 2 μm.

disruption of *CG17218* brings about the *crok* mutant tracheal defects, we used the UAS/GAL4 system to express *CG17218* in the ectoderm of *crok* mutants, driven by the *69B* GAL4 line (*ect>crok*). Such expression restored the tracheal tube size defects of *crok* mutants (Fig. 1D) and produced healthy larvae, providing evidence that *CG17218*/*crok* is a new tracheal tube size gene.

crok mutants have impaired SJ functions and reduced septa

The convoluted dorsal trunks in *crok* mutants are typical for embryos with disrupted SJ components (Wu and Beitel, 2004). Additional characteristics of such SJ mutants are disorganized tracheal luminal chitin matrix and impaired apical localization of the Knickkopf (Knk) protein, which is required for correct chitin matrix assembly (Moussian et al., 2006; Tonning et al., 2005; Wang et al., 2006). Indeed, when staining for chitin and Knk, we found that *crok* mutants also exhibit a similar disorganized luminal chitin matrix, associated with a failure to restrict Knk to the apical surface (Fig. 1E,F).

To directly test whether *crok* is required for SJ functions, we analyzed the paracellular diffusion barrier. A 10-kDa dextran conjugated to a Rhodamine dye was injected into the embryonic body cavity of *crok* mutant and wild-type embryos at stage 16, and the passage of the dye across the tracheal epithelium was assessed. In wild-type embryos, the dye is excluded from the tracheal lumen when analyzed 20 minutes after injection (Fig. 1G) (Lamb et al., 1998). In *crok* mutant embryos, the dye rapidly diffused into the tracheal lumen (Fig. 1H). The dye also leaked into the lumen cavity of the mutant salivary glands (Fig. 1I,J), suggesting that *crok* is required for paracellular barrier functions in both tracheal and salivary gland epithelia. Consistent with the impaired paracellular barrier, transmission electron microscopy (TEM) analyses of stage 16 *crok* mutant embryos revealed reduced and irregular SJs. Although wild-type SJs are seen as ladder-like structures of electron-dense septa between adjacent cell membranes, the mutant tracheal cells formed sparse and less electron-dense septa (Fig. 1K,L). The tracheal cells of *crok* mutants were also seen to contain large unusual vesicle-like structures (Fig. 1M,N), which have previously been observed upon loss of the SJ component Sinu (Wu et al., 2004). Crok is therefore required for paracellular barrier functions and septa formation.

Crok is required for subcellular localization of SJ components

To further understand the basis for the reduced septa in *crok* mutant embryos, we analyzed the subcellular distribution of SJ components in the mutants. The embryos were stained for Nrx-IV, ATPα, Cora, Sinu and the homophilic cell adhesion molecule Fasciclin 3 (Fas3), which is a sensitive marker for SJ integrity (Fig. 2). SJ components begin to accumulate along the apicolateral plasma membrane at stage 14 in the wild-type trachea (Laprise et al., 2009). In *crok* mutants, tracheal cells show defects in plasma membrane accumulation of SJ components already at early stage 15, but the components appear present in the cytoplasm (Fig. 2A). Consistently, comparison of the levels of Nrx-IV and ATPα in extracts from stage 15 wild-type and *crok* mutant embryos on

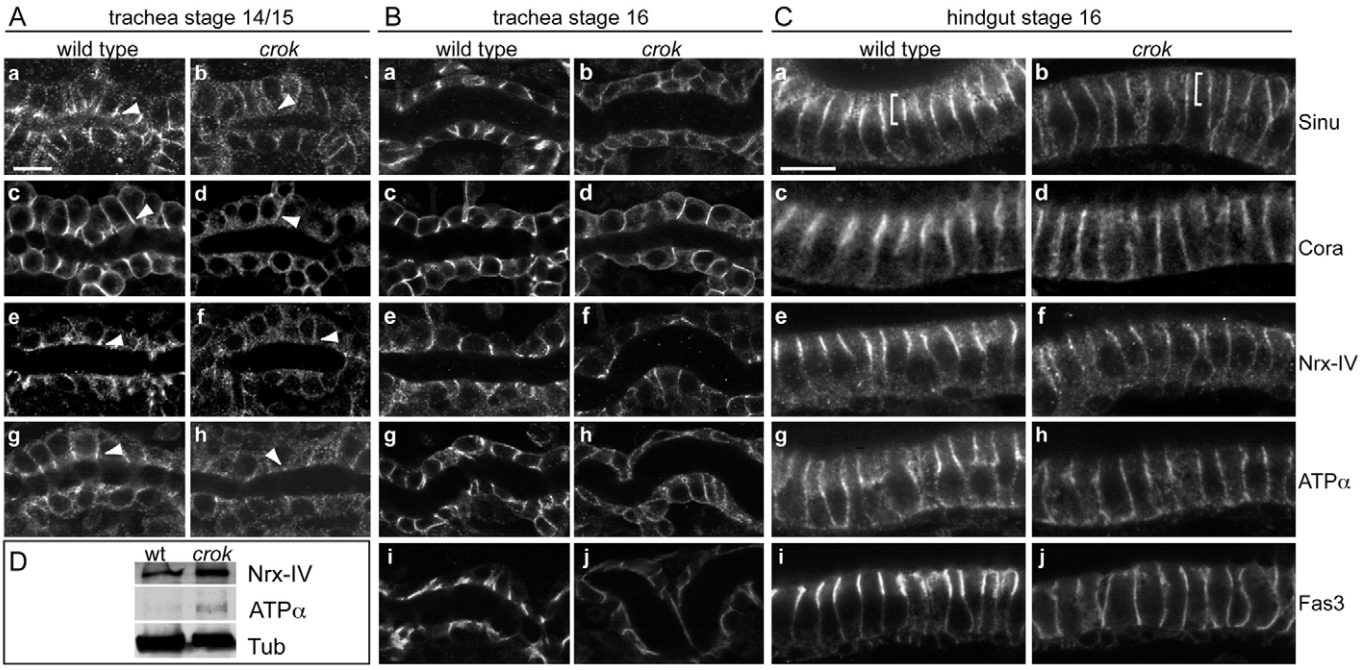

Fig. 2. Crooked is required for correct localization of SJ components. (**Aa-h**,**Ba-j**) Stage 14/15 (A) and stage 16 (B) dorsal trunks from wild-type and *crok*^{KG06053} mutant embryos stained for different SJ components, as indicated (far right). Arrowheads point to the apicolateral membrane region, where SJs normally form. Sinu, Nrx-IV, Cora and ATPα are apical at stage 14/15 in the wild type, but not in the mutants (A). Sinu, Nrx-IV, Cora, ATPα and Fas3 fail to accumulate efficiently at the apicolateral membrane in stage 16 mutant tracheal cells, and their staining appears reduced in the mutants (B). (**Ca-j**) In stage 16 wild-type hindgut epithelia, the SJs localize to the apical third of the lateral membrane (brackets). The SJ components show reduced apical accumulation in the mutants. (**D**) Immunoblot of extracts from stage 15 wild-type (wt) and *crok*^{KG06053} mutant (*crok*) embryos stained with anti-Nrx-IV (top), anti-ATPα (middle) and anti-tubulin (Tub, bottom), showing the presence of Nrx-IV and ATPα in the mutants. Their strong detection in the mutant lane might be due to easier extraction of the proteins from the mutant embryos. Scale bars: in A, 5 μm for A,B; in C, 5 μm.

immunoblots shows that *crok* mutants produce these SJ components (Fig. 2D). At stage 16, the analyzed SJ components appear at low levels along the entire lateral surface of *crok* mutant tracheal cells with little, if any, apical concentration (Fig. 2B). Crok is therefore required for efficient incorporation of SJ components in the apicolateral part of the plasma membrane.

We also analyzed the hindgut epithelium, as SJ components normally show clear accumulation within the apical third of the lateral membrane in these columnar cells (Fig. 2C). Again, the apical staining for SJ components is reduced in *crok* mutant embryos. The strongest effects were observed for Sinu and Fas3, which show almost no apical accumulation in the *crok* mutant hindgut. Intriguingly, only small changes in the distribution of SJ components were seen in the *crok* mutant salivary gland (Fig. 3E-G; data not shown), despite it being leaky to the 10-kDa dextran dye, suggesting that SJ assembly in the salivary glands might involve partly redundant mechanisms. As no other effects on epithelial integrity were observed in *crok* mutants, as assessed by staining for the apical determinants Crumbs (Crb) and Bazooka (Baz), and the adherens junction protein Armadillo (Arm) (Fig. 3A-D; data not shown), we conclude that the requirement for Crok in junction formation is specific to the SJs.

Crok is a Ly6-like protein detected in cytoplasmic puncta during SJ assembly

Crok is predicted to be a small protein of 151 amino acid residues (Fig. 4A). A signal peptide and a short C-terminal transmembrane region together with an omega-site at asparagine^{123} suggest that the protein is GPI-linked (bigPI predictor) (Eisenhaber et al., 1998; Eisenhaber et al., 1999). Structural homology detection using the Phyre web server to search the SCOP database of known 3D structures (Kelley and Sternberg, 2009) predicts that the processed Crok protein contains a three-fingered protein (TFP) fold (Fig. 4B). The TFP fold, originally discovered for snake neurotoxins, consists of three adjacent loops emerging from a hydrophobic palm, and is stabilized by 3-6 disulphide bonds (Galat et al., 2008). The TFP fold is present in several receptors that are tethered to the membrane via GPI-anchorage, like the urokinase/plasminogen activator receptor (uPAR) and the Ly6 protein family. Ly6 proteins contain only a single TFP fold that usually is stabilized by five or six disulfide bridges, also called a LU (Ly-6 antigen/uPA receptor-like) domain. As the TFP fold occurs singly in Crok and contains 10 cysteines, Crok is related to the GPI-linked proteins of the Ly6 family.

crok (*CG17218*) is expressed in ectodermal tissues from stage 11/12 (BDGP). To better understand the pattern of *crok* expression, we performed in situ hybridization. Expression of *crok* is evident in tracheal cells from stage 11, as the cells invaginate from the ectoderm, and ceases in the main dorsal trunks (DT) during stage 15 while remaining in the visceral branches (Fig. 4C,D). *crok* transcripts are also prominent in the epidermis, foregut and hindgut from stage 12 to 15, and thus exhibit a general ectodermal distribution at the time of SJ assembly (Fig. 4D). To address the subcellular localization of Crok, we raised a Crok antiserum. The antiserum appeared to be specific to Crok on western blots (Fig. 4K) and stained wild-type embryos weakly in a pattern reminiscent

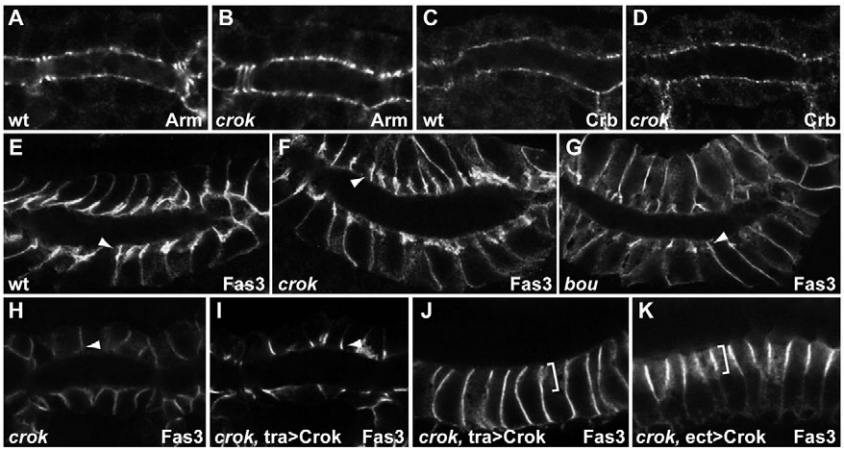

Fig. 3. Crooked acts tissue-autonomously in SJ assembly. (**A-D**) Arm (A,B) and Crb (C,D) appear similar in their expression levels and distribution in wild-type (A,C) and *crok*^{KG06053} mutant (B,D) tracheal cells. (**E-G**) The salivary glands of *crok*^{KG06053} mutants (F) show mild defects in Fas3 distribution when compared with those of wild-type (E) and *bou* mutant (G) embryos. Arrowheads point to the area normally occupied by SJ components. (**H-K**) Fas3 is mislocalized in stage 15 *crok*^{KG06053} mutant tracheal cells (H, arrowhead). In *crok*^{KG06053} embryos that express *UAS-crok* driven by *btl-Gal4* (tra>Crok) the localization is restored in tracheal cells (I, arrowhead), but not in hindgut cells (J, bracket). *crok*^{KG06053} mutant embryos expressing *crok* in the ectoderm, driven by *69B* (O, ect>Crok), show normal Fas3 localization in hindgut cells (K, bracket).

of the *crok* mRNA distribution (Fig. 4E-G). This expression pattern was not detected in *crok* mutant embryos (Fig. 4H), and the antiserum strongly stained embryos that overexpress Crok in the trachea (Fig. 4I), thereby supporting that it has specificity for Crok. Confocal imaging of wild-type tracheal cells revealed a punctate Crok-staining in the cytoplasm, and co-staining for KDEL to mark the endoplasmic reticulum showed that Crok distribution overlaps with, but is not restricted to, this subcellular compartment (Fig. 4J). Intriguingly, no accumulation of Crok was seen at the SJs, as shown by co-staining for Crok and ATPα (Fig. 4L), even when

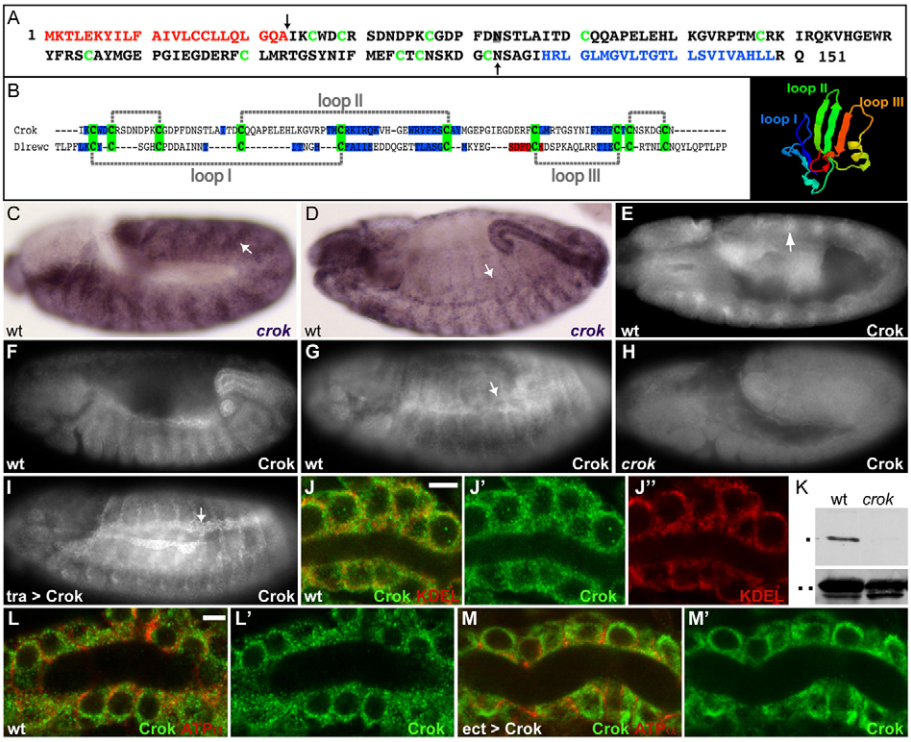

Fig. 4. Crooked is a Ly6-like protein detected in cytoplasm of ectodermal cells. (**A**) Crok has a predicted N-terminal signal peptide (red) (SignalP 3.0 Server), a C-terminal transmembrane region (blue) with an omega-site at Asn^{123} (arrow) for GPI-linkage, and a site for N-glycosylation at Asn^{43} (gray box). The processed protein contains ten cysteines (green). (**B**) Crok is predicted to form a three-fingered protein domain like the BMP receptor IA chain C (D1rewc; right image, modified from the Phyre server). The predicted secondary structure of Crok (top) is aligned with that of D1rewc (below), with beta strands and alpha helices indicated in blue and red, respectively. The ten cysteines of D1rewc are conserved in Crok and form five disulfide bridges (dashed gray lines) with three loops (loop I-III). (**C**,**D**) In situ hybridization reveals *crok* transcripts in the ectoderm and tracheal pockets at stage 11/12 (C; arrow indicates a tracheal metamere), and in the foregut, hindgut, epidermis and trachea at stage 15 (D, arrow indicates a dorsal trunk). (**E-I**) Anti-Crok stains stage 11 tracheal metameres (E, arrow) and stage 13 hindgut, epidermis (F) and tracheal system (G, arrow indicates the dorsal trunk). The staining is absent in *crok*^{KG06053} mutants (H, stage 12), and elevated in the trachea of embryos expressing *UAS-crok* driven by *btl-Gal4* (I, arrow). (**J-J″**) Co-staining for Crok (J′) and KDEL (J″) reveals Crok in cytoplasmic puncta that overlap with the endoplasmic reticulum (J). (**K**) Anti-Crok detects a protein of 17 kDa (single dot) on immunoblots of extracts from wild-type but not *crok*^{KG06053} mutant embryos. Staining for tubulin (two dots) was used as loading control. (**L-M′**) Tracheal cells of wild-type embryos (L) and embryos expressing *UAS-crok* in the ectoderm driven by *69B* (M) labelled with anti-Crok (green; L′,M′) and anti-ATPα (red; merged in L and M) reveal no Crok accumulation at the SJs. Scale bars: in J, 3 μm; in L, 3 μm.

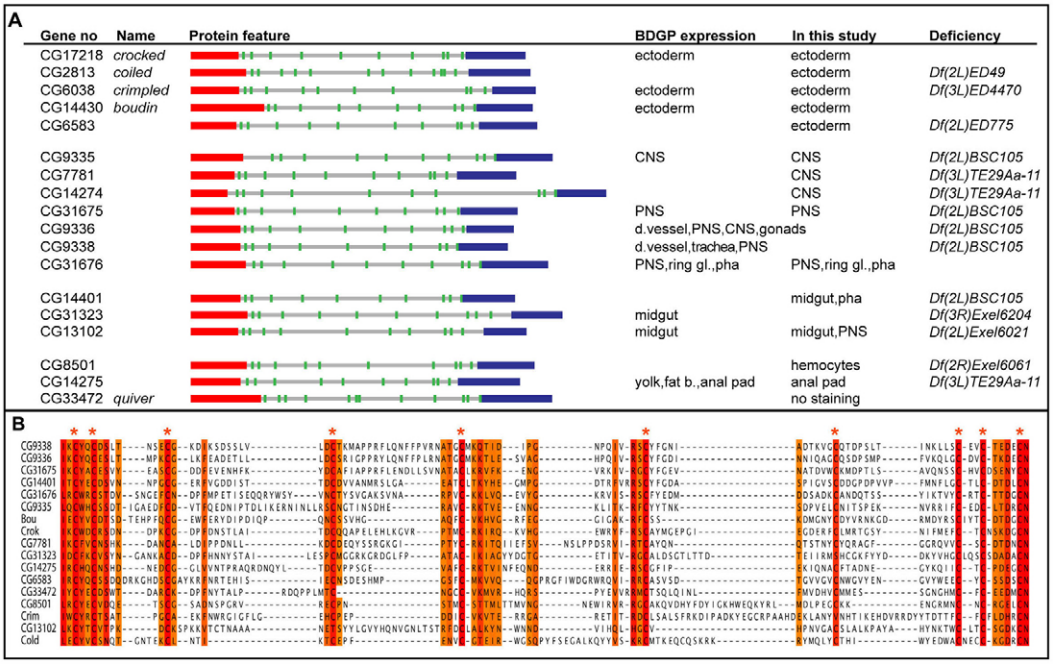

Fig. 5. *Drosophila* Ly6-like proteins with single TFP folds and signal for GPI-linkage. (**A**) The 18 *Drosophila* Ly6-like proteins with predicted GPI-anchorage and a single TFP-domain are drawn in scale with N-terminal signal sequences in red and C-terminal regions removed upon GPI-anchorage in blue. The cysteines are marked in green. All proteins contain 10 cysteines with potential to form five disulfide bridges, except Coiled and Quiver that contain 12 cysteines. The proteins are grouped according to their expression pattern. The deficiency lines used to assess a requirement for each gene in SJ formation are denoted in the left column. (**B**) Multiple alignment (processed in Jalview, using MAFFT running as a web service) (Waterhouse et al., 2009) of the TFP-domain of each Ly6-like protein, except the one encoded by *CG14274* (omitted because of its larger size). The ten conserved cysteines are highlighted with red asterisks.

Crok was overexpressed in the ectoderm (Fig. 4M). The detection of Crok outside the ER was too weak to allow examination of possible colocalization with other vesicle proteins. In further attempts to address Crok subcellular localization, we generated flies that express either FLAG- or GFP-tagged Crok variants, in which the tag was inserted after the N-terminal signal sequence. These proteins displayed a largely perinuclear localization when expressed in epithelial tissues (not shown) similar to endogenously expressed Crok, but unfortunately they could not substitute for wild-type Crok in genetic rescue tests. Together, the results suggest that Crok resides in intracellular membrane compartments, including the ER, presumably assisting the assembly or trafficking of SJ components to or from the plasma membrane.

Crok is similar to Bou, but acts tissue-autonomously in SJ formation

In our screen for new tube size mutants, we found a second mutant with convoluted tracheal tubes and defective SJs (see Fig. S1 in the supplementary material). This mutant carries a P-element (*CG14430*^{GG01077}) in the 3′UTR of *CG14430*, another gene encoding a small GPI-linked protein with 10 cysteines, similar to Crok (see Fig. S1 in the supplementary material). *CG14430* was recently reported to encode a Ly6-like protein required for SJ formation, called Boudin (Bou) (Hijazi et al., 2009). Bou was shown to be secreted and to function non-cell-autonomously in SJ formation. Thus, expression of *bou* in the trachea, driven by the *btl-GAL4* driver, not only rescued the *bou* mutant tracheal phenotype, but also the hindgut defects (Hijazi et al., 2009). By contrast, when Crok was expressed in the trachea of *crok* mutant embryos (*tra>crok*), the tracheal mutant defects were rescued, but no rescuing effects were seen in the hindgut (Fig. 3H-J). Crok expression in the entire ectoderm does, however, also rescue the hindgut defects of *crok* mutants (Fig. 3K), suggesting that Crok functions tissue-autonomously to support SJ assembly.

Additional Ly6-like proteins expressed in the ectoderm

Vertebrate Ly6-like proteins exhibit diverse substrate specificity and tissue expression, but groups of Ly6 proteins have been found to participate in similar biological processes (Bamezai, 2004). Because Crok and Bou are required for SJ formation, we investigated whether additional *Drosophila* Ly6-like proteins might be expressed in SJ-forming tissues with potential roles in SJ assembly. Using position-specific iterative BLAST (PSI-BLAST), including only proteins of 130 to 200 amino acids, we obtained 23 Ly6-like protein sequences apart from Crok and Bou. Two of these, encoded by *CG4363* and *CG15347*, contain 20 cysteines and appear to harbour two TFP domains. By screening the remaining 21 proteins for the presence of a signal peptide and a potential GPI-anchor signal, we found 16 proteins with features similar to those of Crok and Bou (Fig. 5A). All 16 proteins are predicted to form a single TFP fold (Kelley and Sternberg, 2009), and represent a subset of the recently reported Ly6 domain-containing proteins (Hijazi et al., 2009). A multiple sequence alignment of the Ly6-like proteins revealed little primary sequence homology (Fig. 5B). Apart from the ten cysteines (marked by asterisks in Fig. 5B) and a few flanking amino acids, the proteins showed similarity mainly at their N- and C-termini, which is consistent with extensive interactions between the N- and C-terminal sequences seen in TFP domains (Galat et al., 2008).

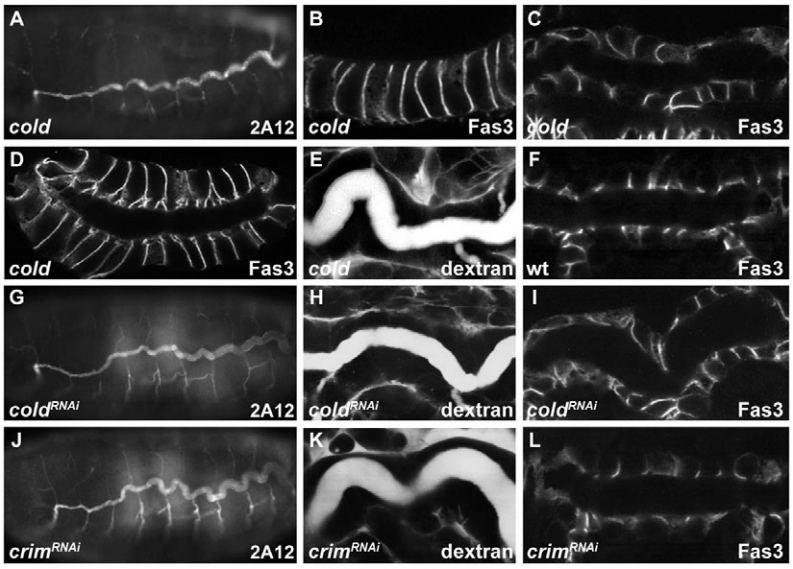

Fig. 6. Crimpled and Coiled are required for SJ formation. (**A-F**) *cold*^{f05607}*/Df(2L)ED49* embryos show convoluted dorsal trunks (A), reduced SJ accumulation of Fas3 in the hindgut (B), trachea (C) and salivary glands (D), and a disrupted tracheal paracellular barrier as assessed by dextran-dye injection (E). The wild-type tracheal Fas3 distribution is shown for comparison (F). (**G-I**) Tracheal expression of *UAS-cold*^{RNAi} using *btl-Gal4* causes convoluted dorsal trunks (G), a disrupted tracheal pararcellular barrier (H) and Fas3 mislocalization in tracheal cells (I). (**J-L**) Tracheal expression of *UAS-crim*^{RNAi} using *btl-Gal4* causes convoluted dorsal trunks (J), a defective tracheal paracellular barrier (K) and mislocalized Fas3 in tracheal cells (L). All images show early stage 16 embryos.

Embryonic RNA expression patterns for nine of the 16 genes are provided by BDGP. We used in situ hybridization to verify the expression of some of these and to establish the expression of the remaining seven genes (see Fig. S2 in the supplementary material), and found that many *Drosophila* Ly6-like genes can be grouped according to their pattern of expression (summarized in Fig. 5A). The three genes, *CG2813*, *CG6038* and *CG6583*, are intriguing, as they are expressed in the ectoderm in a similar pattern to that of *crok* and *bou*. Another three genes show selective expression in the central nervous system (CNS), which forms SJs between glial cells to provide a blood-brain barrier (Stork et al., 2008). Other prominent gene expression domains include the midgut and the peripheral nervous system (PNS) (Fig. 5A; see also Fig. S2 in the supplementary material; the BDGP).

Two Ly6-like proteins, Coiled and Crimpled, are required for SJ formation

In order to test whether additional Ly6 genes might be required for ectodermal SJ formation, we analyzed embryos homozygous for chromosomal deficiencies that uncover the gene of interest. Deficiency lines for nearly all genes were included in this survey (listed in Fig. 5A) to cover for misinterpretations of the expression data and possible non-cell-autonomous gene functions (like *bou*). The deficiency lines were stained with 2A12 to reveal tracheal tube size defects, and with anti-Fas3 to assess SJ integrity.

Two deficiency lines, *Df(2L)ED49* and *Df(2L)ED4470* (deficient for the ectodermally expressed *CG2813* and *CG6038*, respectively) exhibited elongated and convoluted tracheal dorsal trunks in homozygous embryos at stage 16 (see Fig. S3 in the supplementary material). The embryos also show reduced and mislocalized Fas3 staining in ectodermal tissues and failed to prevent the 10-kDa dextran from diffusing across the tracheal epithelium (see Fig. S3 in the supplementary material). A third gene expressed in the ectoderm that also removes *crok*, *CG6583*, was uncovered by *Df(2L)ED775*. However, the tracheal tube size defects of *Df(2L)ED775* were rescued by tracheal expression of *crok* (not shown), suggesting that *CG6583* is not essential for SJ formation. None of the other deficiencies caused tracheal tube size defects.

The requirement for *CG2813* in SJ formation was confirmed through analysis of a lethal piggyBac insertion located within the first intron of *CG2813* (*CG2813*^{f05607}), by gene knockdown using RNA interference (RNAi), and by genetic rescue using a *UAS-CG2813* cDNA transgene. We named the gene *coiled* (*cold*), reflecting its tracheal phenotype. Embryos carrying *cold*^{f05607} in trans to *Df(2L)ED49* developed elongated tracheal dorsal trunks (Fig. 6A), failed to correctly localize Fas3 in the hindgut, trachea and salivary glands (Fig. 6B-D), and showed a compromised tracheal barrier function upon dextran-dye injection (Fig. 6E). RNAi-mediated knockdown of *cold* in the trachea caused similar elongated dorsal trunks, reduced and mislocalized Fas3 in tracheal cells, and a defective tracheal paracellular barrier (Fig. 6G-I).

No known mutant alleles for *CG6038* were available, and instead we obtained an RNAi line for *CG6038* that is reported to have no off targets. RNAi knockdown of *CG6038* in tracheal cells, using *btl-Gal4*, caused tracheal tube size defects, and we called the gene *crimpled* (*crim*) with reference to the tracheal phenotype (Fig. 6J). Tracheal expression of the RNAi line (*crim*^{RNAi}) also caused Fas3 mislocalization in tracheal cells and a compromised paracellular barrier (Fig. 6K,L), suggesting that *crim* is yet another Ly6 protein required for SJ formation. Because the restricted expression of *cold*^{RNAi} and *crim*^{RNAi} in the trachea was able to impair tracheal SJ functions, it appears that the tracheal requirement for Cold and Crim cannot be rescued by secretion of these proteins in other tissues. In support of the notion that *cold* functions autonomously, we found that expression of *UAS-cold* in the dorsal hindgut epithelium of *cold* mutant embryos under the *engrailed-Gal4* driver (*en>cold*) rescued the SJ defects in dorsal cells, but not in cells of the ventral hindgut epithelium (Fig. 7A,B). We conclude that SJ formation requires the non-redundant function of four Ly6-like proteins of which three, Crok, Cold and Crim, function tissue-autonomously.

Cold and Crok are involved in trafficking of the Nrx-IV complex

Our results indicating that Crok is associated with intracellular vesicles, and that SJ components are produced but fail to accumulate at the SJs in *crok* mutants, suggested that Ly6 proteins might have a role in the preassembly or trafficking of SJ components. We therefore examined whether Cold localizes to cytoplasmic puncta, as we had observed for Crok. Unfortunately, attempts to generate anti-Cold antibodies that recognize endogenously expressed protein were unsuccessful. As an

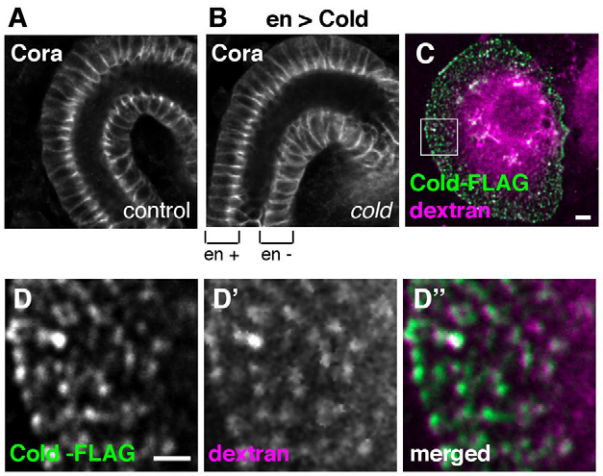

Fig. 7. Coiled acts cell-autonomously and localizes to intracellular vesicles. (**A**,**B**) Anti-Cora labelling of wild-type embryos (A) and embryos in which *UAS-cold* was driven by *engrailed-Gal4* (*en>cold*). Cora is localized to the SJ only in the *en*-expressing cells, which comprise the dorsal half of the hindgut, showing that Cold functions autonomously (B). (**C-D″**) Cold-FLAG colocalizes with dextran-labelled vesicles in S2 cells. The region indicated by a square in C is shown at higher magnification in D-D″. Scale bars: 2 μm in A-C; 1 μm in D-D″.

alternative approach, we expressed epitope-tagged Cold in cultured S2 cells. Flag-tagged Cold protein accumulated in cytoplasmic puncta that partially colocalized with fluid phase-endocyosed dextran (Marchetti et al., 2009) (Fig. 7C,D), suggesting that Cold associates with a vesicular compartment in these cells.

To further explore the effect of Ly6 proteins on SJ assembly, we examined the distribution of Nrx-IV-GFP, expressed under its endogenous promoter, in live embryos. Nrx-IV is a core SJ component that is conserved between flies and mammals (Banerjee et al., 2006). Strikingly, we observed that Nrx-IV-GFP accumulates in cytoplasmic puncta in the embryonic epidermis of *crok* or *cold* mutants (Fig. 8A-C,K), suggesting a defect in some aspect of Nrx-IV trafficking. By contrast, such puncta were only rarely observed in wild-type embryonic epithelial cells (Fig. 8A,K).

To determine whether the Nrx-IV-GFP cytoplasmic puncta observed in *crok* and *cold* mutant embryos are associated with a vesicular compartment, we performed dextran-labelling experiments. Depending on the length of incubation, fluorescent dextran can label multiple compartments, including endosomes, lysosomes and recycling vesicles (Marchetti et al., 2009). Dextran injection into *cold* and *crok* mutant embryos expressing Nrx-IV-GFP revealed an obvious, although not complete, correlation between the Nrx-IV puncta and dextran-labelled vesicles (Fig. 8G,H,L). A similar correlation was seen in *cora* mutant embryos (Fig. 8I,L). By contrast, the rare Nrx-IV-GFP puncta seen in wild-type embryos were much less frequently associated with dextran, suggesting that Nrx-IV trafficking is severely altered in these mutant backgrounds. The large Nrx-IV-GFP puncta in *crok* and *cold* mutants might correspond to the unusual vacuolar structures seen by TEM in embryos mutant for *crok* (Fig. 1N), and could represent late endosomal compartments or lysosomes.

To test whether the vesicular accumulation of Nrx-IV-GFP is a general feature in embryos with defective SJs, we analysed additional SJ mutants. Accumulation of Nrx-IV-GFP in cytoplasmic puncta was evident also in *cora* and *nervana 2* (*nrv2*, the beta subunit of Na^+/K^+ ATPase) embryos, but not in *Gliotactin* (*Gli*) mutants (Fig. 8D-F,K). Moreover, loss of *cold* function did not have a similar effect on either ATPα or Neuroglian (data not shown), suggesting that the puncta observed in *cold* mutants do not contain fully formed SJ protein complexes. However, we did observe Cora staining in these puncta (data not shown), consistent with previous findings that Cora interacts directly with the cytoplasmic tail of Nrx-IV (Ward et al., 1998) and suggesting the presence of a partial complex. Taken together with our observation that they localize to cytoplasmic puncta rather than to the plasma membrane, these results suggest that Crok and Cold have a selective role in assembly or trafficking of the Nrx-IV complex.

DISCUSSION

In this study, we have identified a group of *Drosophila* Ly6-like proteins with specific functions in SJ formation. On the basis of our analyses of these proteins, we propose that they are not integral SJ components, but intracellular proteins that facilitate the correct assembly and incorporation of core SJ components to form stable junctional complexes.

Diverse functions of Ly6 proteins

Ly6 proteins constitute large protein families in both vertebrates and insects. In mammals, they are expressed in cells of hematopoetic origin, the brain, vascular epithelium, kidney tubular epithelium, lung, keratinocytes, stomach, testis and prostate (Bamezai, 2004). Reflecting their differential expression, Ly6 proteins are used in diverse biological processes. Apart from acting as GPI-linked cell accessory proteins of the immune system, vertebrate Ly6 proteins function in the modulation of nicotinic acetylcholine receptors (Choo et al., 2008; Darvas et al., 2009; Grando, 2008; Levitin et al., 2008; Liu et al., 2009), remodelling of the extracellular matrix during skeletal muscle regeneration (Kafadar et al., 2009), self-renewal of erythroid progenitors (Bresson-Mazet et al., 2008), and lipolytic processing of triglyceride-rich lipoproteins by binding lipoprotein lipase (Beigneux et al., 2009). The presence of a GPI-anchor in Ly6 molecules, a lipid anchor that tethers the proteins on the outer leaflet of the membrane, also suggests that Ly6 proteins can aggregate in lipid rafts to alter the activity of associated proteins (Bamezai, 2004; Halova et al., 2002).

We find that the *Drosophila* Ly6-like genes also exhibit a diverse tissue-specific distribution during development, with subsets of genes showing similar tissue expression, suggesting that they participate in similar biological processes. Indeed, five of the 18 *Drosophila* Ly6-like genes are expressed in a similar pattern in the developing ectoderm, and at least four are required for SJ formation, including *bou* (Hijazi et al., 2009), *crok*, *crim* and *cold* (this study). The only other GPI-linked *Drosophila* Ly6 protein studied so far is *quiver* (*qvr*; also known as *sleepless*), which is required for sleep and appears to affect the levels of the voltage-dependent potassium channel Shaker (Koh et al., 2008).

Ly6 proteins in SJ formation

Our phenotypic analyses of *crok* mutants show that Crok is required for plasma membrane accumulation of SJ components. As SJ components were detected in the tracheal cytoplasm of stage 15 *crok* mutant embryos and protein analyses on immunoblots show that ATPα and Nrx-VI are present in *crok* mutants, we conclude that Crok is not required for the synthesis of SJ components.

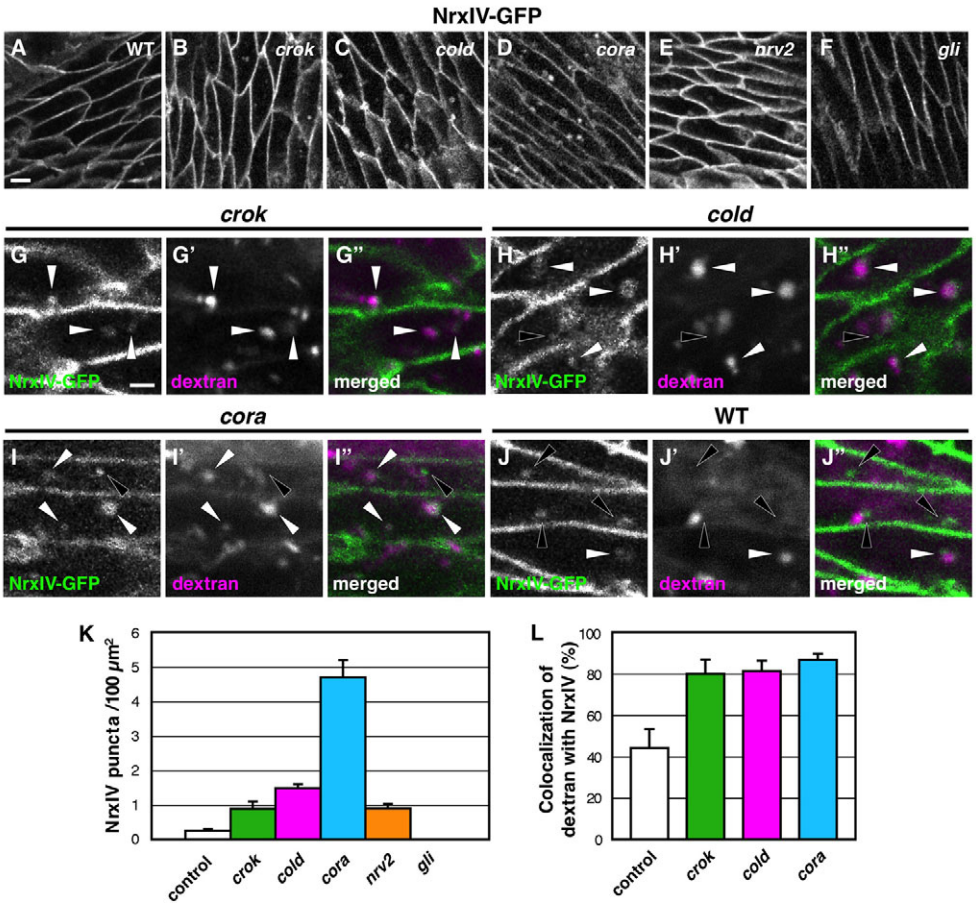

Fig. 8. Crooked and Coiled affect the intracellular trafficking of Nrx-IV. (**A-F**) Distribution of Nrx-IV-GFP in different SJ mutants. Nrx-IV-GFP was observed in the living epidermis of wild-type (A), *crok* (B), *cold* (C), *cora* (D), *nrv2* (E) and *Gli* (F) embryos. Nrx-IV accumulates in cytoplasmic puncta in *crok*, *cold, cora* and *nrv2* mutants, but only rarely in wild-type or *Gli* mutant embryos (F). (**G-J"**) Cytoplasmic Nrx-IV puncta in *crok* (G-G"), *cold* (H-H"), *cora* (I-I") and rarely wild-type (J-J") stage 14-15 embryos colocalize with dextran-labelled vesicles. White and black arrowheads indicate Nrx-IV puncta with and without dextran, respectively. (**K**) To determine the frequency of Nrx-IV-GFP vesicles in the different genotypes, the number of Nrx-IV vesicles was counted in 100 μm^2 regions of the embryonic epidermis. Average values (±s.e.m.) for each genotype are shown. Values for *crok*, *cold*, *cora* and *nrv2* are significantly greater than those for either wild-type or *Gli* embryos ($P<0.005$, Student's *t*-test). (**L**) Percentage of Nrx-IV vesicles that co-label with fluorescent dextran in each of the indicated genotypes (*Gli* mutants were not scored because sufficient Nrx-IV vesicles could not be found in this genotype). Average values for each genotype are shown (error bars indicate s.e.m.). Values for *crok*, *cold* and *cora* are significantly greater than that for wild type ($P<0.05$, Student's *t*-test). Scale bars: 2 µm in A-F; 1 µm in G-J".

Moreover, we found elevated levels of ATPα and Nrx-VI in mutant embryonic extracts, despite an apparent reduction of immunofluorescence staining for these proteins, suggesting that these components are more easily solubilized in the mutant embryos. It thus appears that Crok is required for the formation of SJ complexes at the correct plasma membrane domain.

The function of both Crok and Cold appears to be necessary for the efficient incorporation of Nrx-IV into a stable SJ-associated complex. Upon loss of Crok and Cold, Nrx-IV-GFP accumulates in large intracellular vesicles. A similar situation occurs upon loss of Cora, which interacts with the cytoplasmic tail of Nrx-IV. The presence of fluid-phase dextran in these vesicles suggests that the Nrx-IV-GFP puncta in *crok* and *cold* mutants represent endocytosed protein, possibly on route to degradation in lysosomal compartments. Consistent with this idea, we observed (data not shown) that subsets of the Nrx-IV vesicles in *cold* mutants colocalize with endocytic markers, including Rab5 (early endosomes), Rab11 (recycling endosomes), Hrs (late endosomes) and Dor (lysosomes). As other known SJ components were not detected in these vesicles, it appears that they contain SJ subcomplexes that include Nrx-IV and Cora. This specificity could suggest either that Nrx-IV and interacting proteins are more sensitive than are other components to disruption in SJ assembly, or that Crok and Cold are specifically involved in the stable integration of Nrx-IV and interacting proteins into the SJ complex. Further experiments will be required to discern these alternative possibilities.

Bou, Crok and Cold all appear to accumulate in intracellular membrane compartments. Previous studies have shown that uPAR, an extensively studied GPI-linked protein with two LU domains, is endocytosed and recycled, and that this trafficking is essential for its function (Sturge et al., 2003). Consistent with this idea, we found that Cold colocalizes with dextran-labelled vesicles in cultured cells. In addition, although Bou appears to accumulate in the perinuclear cytoplasm (Hijazi et al., 2009), the non-autonomous behaviour of Bou suggests that it travels to the plasma membrane. Like Bou, Crok shows an apparent association with internal membrane compartments, particularly the ER. The Crok antiserum

does not detect endogenous Crok at high levels, and it is possible that Crok in addition associates transiently with the cell surface. We have so far not been able to conclusively address a possible colocalizaiton of Nrx-IV with Crok or Cold, or with markers for endosomal compartments, and it is currently unclear whether the Ly6 proteins act in the sorting, trafficking or pre-assembly of SJ components prior to their transport to the site of junction assembly, or in an endocytic recycling of the components.

The non-redundant requirement for four Ly6-like proteins in SJ assembly is intriguing and coherent with the need for multiple Ly6-like proteins in the allosteric modulation of nicotinic acetylcholine receptor (nAChR) functions. These Ly6-like proteins include Lynx1 and possibly Lypd6 in neurons, and the secreted proteins Slurp1 and Slurp2 in the ectoderm (Arredondo et al., 2005; Darvas et al., 2009; Hogg et al., 2005; Lester et al., 2009). It has further been suggested that the lynx-nAChR interactions occur during receptor biosynthesis and maturation in the endoplasmic reticulum, a main site for assembly of the multi-subunit membrane proteins of nAChRs (Lester et al., 2009). In analogy, the *Drosophila* Ly6-like proteins might assume roles as allosteric modulators of multiprotein SJ complexes to promote their functional association.

Together, the analyses of Crok, Crim, Cold and Bou highlight a central task for Ly6 proteins in SJ formation that might also be essential for vertebrate paranodal junction assembly. Identification of their ligands and the subcellular site of action should contribute further understanding of how highly ordered, multi-protein complexes form along precise subdomains of the plasma membrane.

Acknowledgements

We thank S. Baumgartner, G. Beitel, S. Luschnig, B. Moussian and A. Wodarz for providing antisera; S. Katz for technical help; members of the R. Fehon and I. Rebay laboratories for comments; and the Centre for Cellular Imaging at the Sahlgrenska Academy, University of Gothenburg for the use of confocal microscopy. The antibodies obtained from DHSB developed under the auspices of the NICHD and maintained by the University of Iowa were developed by M. Krasnow, M. Douglas, E. Wieschaus, E. Knust and C. Goodman. This work was funded by the Swedish Research Council and the Royal Swedish Academy of Sciences to A.E.U., and by the NIH (GM074063) to R.G.F. Deposited in PMC for release after 12 months.

Competing interests statement

The authors declare no competing financial interests.

Supplementary material

Supplementary material for this article is available at
http://dev.biologists.org/lookup/suppl/doi:10.1242/dev.052605/-/DC1

References

Arredondo, J., Chernyavsky, A. I., Webber, R. J. and Grando, S. A. (2005). Biological effects of SLURP-1 on human keratinocytes. *J. Invest. Dermatol.* **125**, 1236-1241.

Bamezai, A. (2004). Mouse Ly-6 proteins and their extended family: markers of cell differentiation and regulators of cell signaling. *Arch. Immunol. Ther. Exp. (Warsz)* **52**, 255-266.

Banerjee, S., Sousa, A. D. and Bhat, M. A. (2006). Organization and function of septate junctions: an evolutionary perspective. *Cell Biochem. Biophys.* **46**, 65-77.

Behr, M., Riedel, D. and Schuh, R. (2003). The claudin-like megatrachea is essential in septate junctions for the epithelial barrier function in Drosophila. *Dev. Cell* **5**, 611-620.

Beigneux, A. P., Weinstein, M. M., Davies, B. S., Gin, P., Bensadoun, A., Fong, L. G. and Young, S. G. (2009). GPIHBP1 and lipolysis: an update. *Curr. Opin. Lipidol.* **20**, 211-216.

Bresson-Mazet, C., Gandrillon, O. and Gonin-Giraud, S. (2008). Stem cell antigen **2**, a new gene involved in the self-renewal of erythroid progenitors. *Cell Prolif.* **41**, 726-738.

Buszczak, M., Paterno, S., Lighthouse, D., Bachman, J., Planck, J., Owen, S., Skora, A. D., Nystul, T. G., Ohlstein, B., Allen, A. et al. (2007). The carnegie protein trap library: a versatile tool for Drosophila developmental studies. *Genetics* **175**, 1505-1531.

Choo, Y. M., Lee, B. H., Lee, K. S., Kim, B. Y., Li, J., Kim, J. G., Lee, J. H., Sohn, H. D., Nah, S. Y. and Jin, B. R. (2008). Pr-lynx1, a modulator of nicotinic acetylcholine receptors in the insect. *Mol. Cell. Neurosci.* **38**, 224-235.

Darvas, M., Morsch, M., Racz, I., Ahmadi, S., Swandulla, D. and Zimmer, A. (2009). Modulation of the Ca2+ conductance of nicotinic acetylcholine receptors by Lypd6. *Eur. Neuropsychopharmacol.* **19**, 670-681.

Eisenhaber, B., Bork, P. and Eisenhaber, F. (1998). Sequence properties of GPI-anchored proteins near the omega-site: constraints for the polypeptide binding site of the putative transamidase. *Protein Eng.* **11**, 1155-1161.

Eisenhaber, B., Bork, P. and Eisenhaber, F. (1999). Prediction of potential GPI-modification sites in proprotein sequences. *J. Mol. Biol.* **292**, 741-758.

Faivre-Sarrailh, C., Banerjee, S., Li, J., Hortsch, M., Laval, M. and Bhat, M. A. (2004). Drosophila contactin, a homolog of vertebrate contactin, is required for septate junction organization and paracellular barrier function. *Development* **131**, 4931-4942.

Fehon, R. G., Dawson, I. A. and Artavanis-Tsakonas, S. (1994). A Drosophila homologue of membrane-skeleton protein 4.1 is associated with septate junctions and is encoded by the coracle gene. *Development* **120**, 545-557.

Galat, A., Gross, G., Drevet, P., Sato, A. and Menez, A. (2008). Conserved structural determinants in three-fingered protein domains. *FEBS J.* **275**, 3207-3225.

Genova, J. L. and Fehon, R. G. (2003). Neuroglian, Gliotactin, and the Na+/K+ ATPase are essential for septate junction function in Drosophila. *J. Cell Biol.* **161**, 979-989.

Girault, J. A. and Peles, E. (2002). Development of nodes of Ranvier. *Curr. Opin. Neurobiol.* **12**, 476-485.

Grando, S. A. (2008). Basic and clinical aspects of non-neuronal acetylcholine: biological and clinical significance of non-canonical ligands of epithelial nicotinic acetylcholine receptors. *J. Pharmacol. Sci.* **106**, 174-179.

Halova, I., Draberova, L. and Draber, P. (2002). A novel lipid raft-associated glycoprotein, TEC-21, activates rat basophilic leukemia cells independently of the type 1 Fc epsilon receptor. *Int. Immunol.* **14**, 213-223.

Han, K. (1996). An efficient DDAB-mediated transfection of Drosophila S2 cells. *Nucleic Acids Res.* **24**, 4362-4363.

Hijazi, A., Masson, W., Auge, B., Waltzer, L., Haenlin, M. and Roch, F. (2009). boudin is required for septate junction organisation in Drosophila and codes for a diffusible protein of the Ly6 superfamily. *Development* **136**, 2199-2209.

Hogg, R. C., Buisson, B. and Bertrand, D. (2005). Allosteric modulation of ligand-gated ion channels. *Biochem. Pharmacol.* **70**, 1267-1276.

Kafadar, K. A., Yi, L., Ahmad, Y., So, L., Rossi, F. and Pavlath, G. K. (2009). Sca-1 expression is required for efficient remodeling of the extracellular matrix during skeletal muscle regeneration. *Dev. Biol.* **326**, 47-59.

Kelley, L. A. and Sternberg, M. J. (2009). Protein structure prediction on the Web: a case study using the Phyre server. *Nat. Protoc.* **4**, 363-371.

Koh, K., Joiner, W. J., Wu, M. N., Yue, Z., Smith, C. J. and Sehgal, A. (2008). Identification of SLEEPLESS, a sleep-promoting factor. *Science* **321**, 372-376.

Lamb, R. S., Ward, R. E., Schweizer, L. and Fehon, R. G. (1998). Drosophila coracle, a member of the protein 4.1 superfamily, has essential structural functions in the septate junctions and developmental functions in embryonic and adult epithelial cells. *Mol. Biol. Cell* **9**, 3505-3519.

Laprise, P., Lau, K. M., Harris, K. P., Silva-Gagliardi, N. F., Paul, S. M., Beronja, S., Beitel, G. J., McGlade, C. J. and Tepass, U. (2009). Yurt, Coracle, Neurexin IV and the Na(+),K(+)-ATPase form a novel group of epithelial polarity proteins. *Nature* **459**, 1141-1145.

Lester, H. A., Xiao, C., Srinivasan, R., Son, C. D., Miwa, J., Pantoja, R., Banghart, M. R., Dougherty, D. A., Goate, A. M. and Wang, J. C. (2009). Nicotine is a selective pharmacological chaperone of acetylcholine receptor number and stoichiometry. Implications for drug discovery. *AAPS J.* **11**, 167-177.

Levitin, F., Weiss, M., Hahn, Y., Stern, O., Papke, R. L., Matusik, R., Nandana, S. R., Ziv, R., Pichinuk, E., Salame, S. et al. (2008). PATE gene clusters code for multiple, secreted TFP/Ly-6/uPAR proteins that are expressed in reproductive and neuron-rich tissues and possess neuromodulatory activity. *J. Biol. Chem.* **283**, 16928-16939.

Liu, Z., Cao, G., Li, J., Bao, H. and Zhang, Y. (2009). Identification of two Lynx proteins in Nilaparvata lugens and the modulation on insect nicotinic acetylcholine receptors. *J. Neurochem.* **110**, 1707-1714.

Llimargas, M., Strigini, M., Katidou, M., Karagogeos, D. and Casanova, J. (2004). Lachesin is a component of a septate junction-based mechanism that controls tube size and epithelial integrity in the Drosophila tracheal system. *Development* **131**, 181-190.

Marchetti, A., Lelong, E. and Cosson, P. (2009). A measure of endosomal pH by flow cytometry in Dictyostelium. *BMC Res. Notes* **2**, 7.

Moussian, B., Tang, E., Tonning, A., Helms, S., Schwarz, H., Nusslein-Volhard, C. and Uv, A. E. (2006). Drosophila Knickkopf and Retroactive are needed for epithelial tube growth and cuticle differentiation through their specific requirement for chitin filament organization. *Development* **133**, 163-171.

Paul, S. M., Ternet, M., Salvaterra, P. M. and Beitel, G. J. (2003). The Na+/K+ ATPase is required for septate junction function and epithelial tube-size control in the Drosophila tracheal system. *Development* **130**, 4963-4974.
Stork, T., Engelen, D., Krudewig, A., Silies, M., Bainton, R. J. and Klambt, C. (2008). Organization and function of the blood-brain barrier in Drosophila. *J. Neurosci.* **28**, 587-597.
Sturge, J., Wienke, D., East, L., Jones, G. E. and Isacke, C. M. (2003). GPI-anchored uPAR requires Endo180 for rapid directional sensing during chemotaxis. *J. Cell Biol.* **162**, 789-794.
Tepass, U. and Hartenstein, V. (1994). The development of cellular junctions in the Drosophila embryo. *Dev. Biol.* **161**, 563-596.
Tepass, U., Tanentzapf, G., Ward, R. and Fehon, R. (2001). Epithelial cell polarity and cell junctions in Drosophila. *Annu. Rev. Genet.* **35**, 747-784.
Tomancak, P., Beaton, A., Weiszmann, R., Kwan, E., Shu, S., Lewis, S. E., Richards, S., Ashburner, M., Hartenstein, V., Celniker, S. E. et al. (2002). Systematic determination of patterns of gene expression during Drosophila embryogenesis. *Genome Biol.* **3**, RESEARCH0088.
Tonning, A., Hemphala, J., Tang, E., Nannmark, U., Samakovlis, C. and Uv, A. (2005). A transient luminal chitinous matrix is required to model epithelial tube diameter in the Drosophila trachea. *Dev. Cell* **9**, 423-430.
Wang, S., Jayaram, S. A., Hemphala, J., Senti, K. A., Tsarouhas, V., Jin, H. and Samakovlis, C. (2006). Septate-junction-dependent luminal deposition of chitin deacetylases restricts tube elongation in the Drosophila trachea. *Curr. Biol.* **16**, 180-185.
Ward, R. E. T., Lamb, R. S. and Fehon, R. G. (1998). A conserved functional domain of Drosophila coracle is required for localization at the septate junction and has membrane-organizing activity. *J. Cell Biol.* **140**, 1463-1473.
Waterhouse, A. M., Procter, J. B., Martin, D. M., Clamp, M. and Barton, G. J. (2009). Jalview Version 2-a multiple sequence alignment editor and analysis workbench. *Bioinformatics* **25**, 1189-1191.
Wu, V. M. and Beitel, G. J. (2004). A junctional problem of apical proportions: epithelial tube-size control by septate junctions in the Drosophila tracheal system. *Curr. Opin. Cell Biol.* **16**, 493-4499.
Wu, V. M., Schulte, J., Hirschi, A., Tepass, U. and Beitel, G. J. (2004). Sinuous is a Drosophila claudin required for septate junction organization and epithelial tube size control. *J. Cell Biol.* **164**, 313-323.
Wu, V. M., Yu, M. H., Paik, R., Banerjee, S., Liang, Z., Paul, S. M., Bhat, M. A. and Beitel, G. J. (2007). Drosophila Varicose, a member of a new subgroup of basolateral MAGUKs, is required for septate junctions and tracheal morphogenesis. *Development* **134**, 999-1009.

Table S1. Oligonucleotides used to generate DNA templates for in vitro transcription

Gene ID	Forward primer	Reverse primer
CG6579	TTAATTACTTGTGATCCACAGACC	GCATTTCTGGACCGGATTT
CG9338	CAAATCGTGAGGTCCTGCTA	TTCCCAACAGCAAGTTCGAT
CG9336	GCTCATCCAAACCAAACAATTT	TAAGATCTAGGCCAGCAGACG
CG14401	CGCACGTTCAGTTCAGTTTC	CCCGAAAACAGTTGATTCCA
CG6329	GTGAACTGCAGCAAACAGGA	TGGTGCAGGAGCAGTAGATG
CG31675	ATTTCACGCTCCACATTTCC	CGTGCGTAAGATCGTCAGAG
CG31676	CATTTTCAGTCTACGGCAAGC	CTTTGGCTCATTTGCACAGC
CG13102	GTAGATAGCAGCGCACCACA	ACGGAGGTCCTCATCTTCCT
CG6038	AGCCAGGGAAACAATCACAC	GCAGGGCAGGAATTAGAGTG
CG9335	CCGCATACACATTGAAAGCA	AATCGACCTGGGGATCTTTT
CG8501	ATGAGTGGATCAGGGTGAGG	TCCGGGAACTGGTAGAACAC
CG31323	TTGATGGCTG CCCAGGTA	ATATTTCCGCCTGCCTCTTC
CG2813	GACTTTGGGCCACACCTTTA	GGGTGCAGTACAGCTGCATA
CG8861	CCACTTGTGGTTGATCGAGA	CTTGGTCAAATGGCTGGATT
CG4363	CATTTCAATTCCCCACAAGG	GAATGAAGCGGTTCCCTAAA
CG15347	TGTACAAGTTCGGCGACAAG	ACTCTGGCCGTCGTTACATC
CG14275	ATTCGCATGACAACGAGGAT	GGGACAGGTGCAAATGATCT
CG14274	GGAATCGCAACCAAAACAAG	CAGCGACATTGCACTCAAAT
CG7781	GCCGTGTGATTAGGACCTGT	CGAAAGAAAAACTG GGTGGA
CG6583	CTGGGGAGTCTACGAAAACG	TGGACGGAATGTGTTTTTGA
CG14430	CTTTCAAGCCTTGCTCTCGT	CCTTCGAACTGCAGAACCTC

The T7 polymerase sequence (TAATACGACTCACTATAGG) was added to each reverse primer in order to enable generation of antisense RNA, and the T3 polymerase sequence (AATTAACCCTCACTAAAGG) was added to the forward primers to enable generation of sense RNA.